Wireless Pers Commun
DOI 10.1007/s11277-009-9776-2

Cyclostationarity-Based Modulation Classification of Linear Digital Modulations in Flat Fading Channels

Octavia A. Dobre · Ali Abdi · Yeheskel Bar-Ness · Wei Su

Abstract Modulation classification is an intermediate step between signal detection and demodulation, and plays a key role in various civilian and military applications. In this correspondence, higher-order cyclic cumulants (CCs) are explored to discriminate linear digital modulations in flat fading channels. Single- and multi-antenna CC-based classifiers are investigated. These benefit from the robustness of the CC-based features to unknown phase and timing offset. Furthermore, the latter provides significant performance improvement due to spatial diversity used to combat the fading effect. Classifier performances are investigated under a variety of channel conditions. In addition, analytical closed-form expressions for the cyclic cumulant polyspectra of linearly digitally modulated signals affected by fading, carrier frequency and timing offsets, and additive Gaussian noise are derived, along with a condition for the oversampling factor to avoid aliasing in the cycle and spectral frequency domains.

Keywords Antenna arrays · Automatic modulation classification · Cycle aliasing · Higher-order cyclic statistics · Probability of correct classification · Selection combining

Part of this work was published in a preliminary form and presented at the IEEE Military Communication Conference (MILCOM) 2003 and 2005, USA, under the titles "Higher-order cyclic cumulants for high order modulation classification," and "Selection combining for modulation recognition in fading channels," respectively.

O. A. Dobre (✉)
Faculty of Engineering and Applied Science, Memorial University of Newfoundland,
St. John's, NL, A1B 3X5, Canada
e-mail: odobre@mun.ca
URL: www.engr.mun.ca/~dobre

A. Abdi · Y. Bar-Ness
Department of Electrical and Computer Engineering, New Jersey Institute of Technology,
Newark, NJ 07102, USA

W. Su
RDECOM, Fort Monmouth, NJ 07703, USA

Published online: 22 July 2009

Abbreviations

ASK	Amplitude shift keying
AWGN	Additive white Gaussian noise
BPSK	Binary phase shift keying
CC	Cyclic cumulant
CF	Cycle frequency
CCP	Cyclic cumulant polyspectrum
FB	Feature based
FIR	Finite impulse response
LB	Likelihood based
MC	Modulation classification
OFDM	Orthogonal frequency division multiplexing
PSK	Phase shift keying
QAM	Quadrature amplitude modulation
QPSK	Quadrature PSK
SNR	Signal-to-noise ratio

1 Introduction

Automatic modulation classification (MC) is a problem of current and future significance for both commercial and military communication systems. In an adaptive communication system, the modulation format can be changed according to the channel state to achieve high efficiency communication. Usually supplementary information about the modulation format is transmitted. However, blind techniques can be used instead in a flexible intelligent receiver, such as software-defined radio, to increase the transmission efficiency. Furthermore, MC represents a critical component of new cognitive radio systems that improve spectral efficiency by adapting their transmission according to their spectral environment [1,2]. In military communication systems, advanced techniques are required for real-time signal interception and processing, which are vital for tactical decision making. A major task of such systems is the automatic recognition of the modulation format of an incoming signal [3]. The design of a modulation classifier essentially involves two steps: signal preprocessing and proper selection of the classification algorithm. Preprocessing tasks may include noise reduction, estimation of carrier frequency, symbol period, signal power, etc. Depending on the classification algorithm chosen in the second step, different preprocessing tasks are required. For the second step, two general classes of MC algorithms can be crystallized, which rely on likelihood based (LB) techniques [4–7], or feature-based (FB) methods [8–18]. In the LB approach, MC is treated as a multiple composite hypothesis testing problem, and computation of the likelihood function of the received signal is required. The complexity of the optimal LB solution has resulted in suboptimal classifiers [5–7]. In the FB approach, on the other hand, several discriminant features are selected and a decision is made based on their observed values. Usually, these features are selected in an ad-hoc way.

In this correspondence we use higher-order cyclic cumulants (CCs) of the baseband intercepted signal as powerful features for linear digital MC, due to their attractive properties. CCs inherit the useful property of cumulants, which is the mathematical convenience of calculating the higher-order cumulants of the sum of independent processes, which is difficult to do for the moments [19–21]. Furthermore, they take advantage of the intrinsic cyclostationarity of communication signals, which makes them robust to interference and stationary noise [20,21].

Relevant MC papers based on cumulants and CCs of the received signal are briefly reviewed in the sequel. Swami and Sadler [8] proposed a hierarchical classifier using features based on the fourth-order cumulants of the baseband sequence, to identify amplitude shift keying (ASK), phase shift keying (PSK) and quadrature amplitude modulation (QAM) signals. In the work of Marchand et al. [9], a feature based on fourth- and second-order CCs was used for quadrature PSK (QPSK), 16-QAM and 64-QAM signal classification. Spooner [10,11] employed CC-based features, with order up to six, for the classification of PSK, QAM, and minimum shift keying signals. Features based on fourth-, sixth-, and eighth-order CCs were proposed in [12] to classify rectangular QAM signals. First- and second-order CC-based features were used in [13] and [14] to identify the modulation format of frequency shift keying signals and discriminate orthogonal frequency division multiplexing (OFDM), single carrier linear digital modulations, and cyclically prefixed single carrier linear digital modulations, respectively. Second-order cyclostationarity was also exploited for the identification of OFDM, code division multiple access, and global system for mobile communication signals [15]. Additive white Gaussian noise (AWGN) channel has been mainly considered in these papers [8–14]. However, in a practical wireless communication scenario, systems are subject to fading as well. In this correspondence we tackle the problem of classifying a large pool of single carrier linearly digitally modulated signals in a flat fading channel, by using eighth-order CC-based features and exploiting spatial diversity to mitigate the impact of fading. Analytical closed-form expressions for the cyclic cumulant polyspectra (CCPs) of linearly digitally modulated signals affected by fading, carrier frequency and timing offsets, and additive Gaussian noise are derived, along with a necessary and sufficient condition for the oversampling factor to avoid aliasing in the cycle and spectral frequency domains.

The correspondence is organized as follows. In Sect. 2 we characterize the signals of interest. Single- and multiple-antenna CC-based classifiers are developed in Sects. 3 and 4, respectively. Simulation results are presented in Sect. 5, and conclusions are drawn in Sect. 6. Definitions of cumulants and CCs, and their sample estimators are introduced in Appendix "1". Derivations of the analytical closed-form expressions for the higher-order CCs and cycle frequencies (CFs), and CCPs are presented in Appendices "2" and "4", respectively. Examples of CCs and CFs are given for illustration in Appendix "3". Finally, Appendix "5" provides the derivation of the condition for the oversampling factor to avoid aliasing in the cycle and spectral frequency domains. Note that results presented in this paper have been partially presented by authors in [16] and [17].

2 Signal Model and its Cyclic Characteristics

If a linearly digitally modulated signal is transmitted through a flat block-fading channel with AWGN, the output of the receive filter is a baseband waveform given by

$$y^{(i)}(t) = \alpha e^{j\varphi} e^{j2\pi \Delta f t} \sum_k s_k^{(i)} p(t - kT - \varepsilon T) + w(t), \tag{1}$$

where α is the channel amplitude, φ is the channel phase (which includes the carrier phase offset), Δf is the carrier frequency offset, T is the symbol period, $0 \leq \varepsilon < 1$ represents the timing offset, $w(t)$ is the zero-mean complex baseband Gaussian noise, $p(t)$ is the combined impulse response of transmit and receive filters in cascade, and $s_k^{(i)}$ represents the symbol transmitted within the k-th period, coming from the i-th modulation format, $i = 1, \ldots, N_{\text{mod}}$. For each i, the data symbols $\{s_k^{(i)}\}$ are assumed to be zero-mean independent and identically

distributed random variables, taken from M_i constellation points. For alphabets of linear digital modulations, see for example, [22] Chap. 4. Without loss of generality, unit variance constellations are considered in the sequel, i.e., $\mathrm{E}[|s_k^{(i)}|^2] = M_i^{-1}\sum_{m=1}^{M_i}|s_m^{(i)}|^2 = 1, i = 1,\ldots,N_{\mathrm{mod}}$, where E[.] is the mathematical expectation. By oversampling the signal $y^{(i)}(t)$ at a rate $f_s = \rho/T$, with ρ as a positive integer representing the oversampling factor, the discrete-time data $y^{(i)}(m) = y^{(i)}(t)|_{t=mT/\rho}$ is obtained.

The nth-order/q-conjugate CC of $y^{(i)}(t)$, at CF $\tilde{\gamma}$ and delay vector $\tilde{\tau}$, and the set of CFs are given, respectively as (see Appendix "2")

$$\tilde{c}_y^{(i)}(\tilde{\gamma};\tilde{\boldsymbol{\tau}})_{n,q} = \alpha^n c_{s^{(i)},n,q} T^{-1} e^{-j2\pi\tilde{\beta}\varepsilon T} e^{j(n-2q)\varphi} e^{j2\pi\Delta f\sum_{u=1}^{n-1}(-)_u\tilde{\tau}_u} \times \int_{-\infty}^{\infty} p^{(*)_n}(t)\prod_{u=1}^{n-1} p^{(*)_u}(t+\tilde{\tau}_u)\, e^{-j2\pi t\tilde{\beta}}dt, \quad q=0,\ldots,n, \tag{2}$$

$$\tilde{\kappa}_{n,q} = \left\{\tilde{\gamma} : \tilde{\gamma} = \tilde{\beta} + (n-2q)\Delta f, \tilde{\beta} = k/T, k \text{ integer}, \tilde{c}_y^{(i)}\left(\tilde{\gamma};\tilde{\boldsymbol{\tau}}\right)_{n,q} \neq 0\right\}, \tag{3}$$

where $\tilde{\boldsymbol{\tau}} = [\tilde{\tau}_1,\ldots,\tilde{\tau}_{n-1}]^{\dagger}$, with $\dagger$ as the transpose, $c_{s^{(i)},n,q}$ is the nth-order/q-conjugate cumulant of the i-th constellation, $(*)_u$ represents a possible conjugation of the u-th term so that the total number of conjugations is $q, u = 1,\ldots,n$, and $(-)_u$ is the minus sign coming from the conjugation $(*)_u, u = 1,\ldots,n-1$. As $w(t)$ is a stationary, zero-mean Gaussian process, its cumulants are time independent, and non-zero only for the second order. Since higher-order ($n \geq 3$) CCs of $y^{(i)}(t)$ are of our interest, the noise contribution does not appear in (2). It should be noted that (2) holds only for a certain delay range (see Appendix "2" for details) and CFs given in (3); otherwise, the CC is zero. As one can easily notice from (2), the timing offset ε, channel phase φ, and carrier frequency offset Δf yield a rotation of the CC. Moreover, the CC is directly proportional to the nth power of the signal amplitude, nth-order/q-conjugate cumulant of the signal constellation, inverse of the symbol period, and functional $\Xi(n,q,\tilde{\tau},\tilde{\beta},p(t)) = \int_{-\infty}^{\infty} p^{(*)_n}(t)\prod_{u=1}^{n-1} p^{(*)_u}(t+\tilde{\tau}_u)\, e^{-j2\pi t\tilde{\beta}}dt$. This functional depends on the order n, number of conjugations q, delay-vector $\tilde{\tau}$, frequency $\tilde{\beta}$, and pulse shape $p(t)$. It can be easily shown that for the commonly-used raised cosine pulse shape, the maximum of $|\Xi(n,q,\tilde{\tau},\tilde{\beta},p(t))|$ is achieved at zero delay vector, $\tilde{\boldsymbol{\tau}} = \mathbf{0}_n$, for any n, q, and $\tilde{\beta}$ (overlapping of the pulse shape factors occurs over their entire support), and this maximum decreases with $\tilde{\beta}$, for any n and q.

The nth-order/q-conjugate CCP of $y^{(i)}(t)$, at CF $\tilde{\gamma}$ and spectral frequency vector $\tilde{\mathbf{f}}$, can be shown to be given by (see Appendix "4")

$$\tilde{C}_y^{(i)}(\tilde{\gamma};\tilde{\mathbf{f}})_{n,q} = \alpha^n c_{s^{(i)},n,q} T^{-1} e^{-j2\pi\tilde{\beta}\varepsilon T} e^{j(n-2q)\varphi} P^{(*)_n}((-)_n(\tilde{\beta} - \sum_{u=1}^{n-1}(-)_u((-)_u\tilde{f}_u - \Delta f))) \times \prod_{u=1}^{n-1} P^{(*)_u}((-)_u\tilde{f}_u - \Delta f), \quad \tilde{\beta} = k/T, \quad k \text{ integer}, \quad q=0,\ldots,n, \tag{4}$$

where $\tilde{\mathbf{f}} = [\tilde{f}_1,\ldots,\tilde{f}_{n-1}]^{\dagger}$ and $P(\tilde{f})$ is the Fourier transform of $p(t)$.

Equations (2)–(4) are valid for any pulse shape. For the raised cosine pulse shape, we derive the actual set $\tilde{\kappa}_{n,q}$ of CFs, which is shown to be essentially limited by the signal bandwidth, and a condition for the oversampling factor to avoid aliasing in the cycle and spectral frequency domains (see Appendix "5"). By using (4) and the fact that $P(\tilde{f})$ is band-limited to $B_p = (1+r)/(2T)$, with r as the roll-off factor, $0 \leq r \leq 1$ (for definition see, e.g., [22] Chap. 9), the following results are obtained: The set of values for $\tilde{\beta}$ in $\tilde{\kappa}_{n,q}, n$

even, is given by $\{\tilde{\beta}\}_n = \{0, \ldots, \pm(n/2-1)/T\}$ for $r = 0$, and includes $\{0, \ldots, \pm n/(2T)\}$ for any $0 < r \leq 1$. Additional values for $\tilde{\beta}$ can exist for certain ranges of r. If $2m/n < r \leq (2m+2)/n, \quad m = 1, \ldots, n/2-1$, the set of additional values for $\tilde{\beta}$ is $\{\pm(n+2)/(2T), \ldots, \pm(n+2m)/(2T)\}$. With $\{\tilde{\beta}\}_n$ as previously mentioned, the set $\tilde{\kappa}_{n,q}$ of CFs is given by (3) if $c_{s^{(i)},n,q} \neq 0$. Otherwise, this is an empty set. Note that $c_{s^{(i)},n,q} = 0$ for n odd and $q = 0, \ldots, n$ [16], which means that the nth-order CCs are zero and, therefore, there is no cycle frequency; For n even and $c_{s^{(i)},n,q} \neq 0$, the necessary and sufficient condition for the oversampling factor ρ to eliminate aliasing is $\rho \geq n-1$ if $r = 0$, and $\rho \geq n+2m+1$ if $2m/n < r \leq (2m+2)/n, m = 0, \ldots, n/2-1$.

When no aliasing occurs, the nth-order/q-conjugate CCs and CCPs of the discrete-time signal $y^{(i)}(m)$, and corresponding set of CFs, are respectively given by [23]

$$c_y^{(i)}(\gamma; \boldsymbol{\tau})_{n,q} = \tilde{c}_y^{(i)}\left(\gamma f_s; \boldsymbol{\tau} f_s^{-1}\right)_{n,q}, \tag{5}$$

$$C_y^{(i)}(\gamma; \mathbf{f})_{n,q} = f_s^{n-1}\tilde{C}_y^{(i)}(\gamma f_s; \mathbf{f} f_s)_{n,q}, \tag{6}$$

$$\kappa_{n,q} = \{\gamma \in [0; 1) : \gamma = \tilde{\gamma}T/\rho, c_y^{(i)}(\gamma; \boldsymbol{\tau})_{n,q} \neq 0\}, \tag{7}$$

where $\boldsymbol{\tau} = \tilde{\boldsymbol{\tau}}\rho/T$ and $\mathbf{f} = \tilde{\mathbf{f}}T/\rho$, with their components given by $\tau_u = \tilde{\tau}_u\rho/T$ and $f_u = \tilde{f}_u T/\rho$, $f_u \in [0, 1)$, respectively. Based on (2) and (5), the explicit expression for the nth-order/q-conjugate CCs of the sampled signal $y^{(i)}(m)$, at CF γ and delay vector τ, can be easily written as

$$\begin{aligned} c_y^{(i)}(\gamma; \boldsymbol{\tau})_{n,q} = {} & \alpha^n c_{s^{(i)},n,q}\rho^{-1}e^{-j2\pi k\varepsilon}e^{j(n-2q)\varphi}e^{j2\pi\Delta f T\rho^{-1}\sum_{u=1}^{n-1}(-)_u\tau_u} \\ & \times \sum_m p^{(*)_n}(m)\prod_{u=1}^{n-1}p^{(*)_u}(m+\tau_u)e^{-j2\pi\beta m}, \end{aligned} \tag{8}$$

where $\gamma = \beta + (n-2q)\Delta f T\rho^{-1}$, $\beta = \tilde{\beta}T\rho^{-1} = k\rho^{-1}$, k integer, $p(m) = p(t)|_{t=mT/\rho}$, and $p(m+\tau_u) = p(t+\tilde{\tau}_u)|_{t=mT/\rho, \tilde{\tau}_u=\tau_u T/\rho}$, $u = 1, \ldots, n-1$. As previously discussed, for the raised cosine pulse shape, the k values actually belong to a finite set that depends on the signal bandwidth (through the roll-off factor) and order n.

3 Single-Antenna Cyclic Cumulant-Based Classifier in Fading Channel

It is clear from (8) that the timing offset ε, channel phase φ, and carrier frequency offset Δf rotate the CC of the signal. Therefore, we take the absolute value of (8)

$$|c_y^{(i)}(\gamma; \boldsymbol{\tau})_{n,q}| = \alpha^n |c_{s^{(i)},n,q}|\rho^{-1}| \sum_m p^{(*)_n}(m)\prod_{u=1}^{n-1}p^{(*)_u}(m+\tau_u)e^{-j2\pi\beta m}|. \tag{9}$$

As one can easily notice, the magnitude of the nth-order/q-conjugate CCs is directly proportional to the magnitude of the nth-order/q-conjugate cumulant, $|c_{s^{(i)},n,q}|$. The theoretical values of $c_{s^{(i)},n,q}$, for $n = 2, 4, 6, 8$, $q = 0, \ldots, n/2$, and 4-ASK, 8-ASK, binary PSK (BPSK), QPSK, 8-PSK, 16-PSK, 16-QAM, 32-QAM, and 64-QAM signals, are given in Table 1. These values are computed using the moment to cumulant formula, in which the moments are calculated for noise-free constellations with unit variance and equiprobable symbols (see Appendix "1"). Note that due to the symmetry of the signal constellations, the nth-order moments and cumulants for odd n are zero, whereas for n even we have $c_{s^{(i)},n,q} = c_{s^{(i)},n,n-q}$.

Table 1 Theoretical cumulants of the unit signal constellations considered in this correspondence

$c_{s^{(i)},n,q}/i$	4-ASK	8-ASK	BPSK	QPSK	8-PSK	16-PSK	16-QAM	32-QAM	64-QAM
$c_{s^{(i)},2,0}$	1	1	1	0	0	0	0	0	0
$c_{s^{(i)},2,1}$	1	1	1	1	1	1	1	1	1
$c_{s^{(i)},4,0}$	−1.36	−1.2381	−2	1	0	0	−0.68	−0.19	−0.619
$c_{s^{(i)},4,1}$	−1.36	−1.2381	−2	0	0	0	0	0	0
$c_{s^{(i)},4,2}$	−1.36	−1.2381	−2	−1	−1	−1	−0.68	−0.69	−0.619
$c_{s^{(i)},6,0}$	8.32	7.1889	16	0	0	0	0	0	0
$c_{s^{(i)},6,1}$	8.32	7.1889	16	−4	0	0	2.08	0.57	1.7972
$c_{s^{(i)},6,2}$	8.32	7.1889	16	0	0	0	0	0	0
$c_{s^{(i)},6,3}$	8.32	7.1889	16	4	4	4	2.08	2.11	1.7972
$c_{s^{(i)},8,0}$	−111.8464	−92.018	−272	−34	1	0	−13.9808	−1.9926	−11.5022
$c_{s^{(i)},8,1}$	−111.8464	−92.018	−272	0	0	0	0	0	0
$c_{s^{(i)},8,2}$	−111.8464	−92.018	−272	34	0	0	−13.9808	−3.8446	−11.5022
$c_{s^{(i)},8,3}$	−111.8464	−92.018	−272	0	0	0	0	0	0
$c_{s^{(i)},8,4}$	−111.8464	−92.018	−272	−34	−33	−33	−13.9808	−13.7862	−11.5022

The fourth-order cumulants of 4-ASK, 8-ASK, BPSK, QPSK, 8-PSK, 16-PSK, 16-QAM, and 64-QAM are given in [8] and the fourth- and sixth-order cumulants of QPSK, 8-PSK, 16-QAM, and 64-QAM in [11]

One can notice from Table 1 that for M-PSK signals, $c_{s^{(i)},M,0}$ is the lowest-order cumulant which can be used to distinguish between M-PSK and M'-PSK ($M' > M$), e.g., the lowest-order statistic to discriminate between 8-PSK and 16-PSK is of order eight. For M-QAM signals $c_{s^{(i)},n,q} = 0$ if $n = 4m$(m integer) and q odd, or $n \neq 4m$ and q even. As expected, for real-valued constellations (4-ASK, 8-ASK and BPSK in Table 1), the nth-order cumulant $c_{s^{(i)},n,q}$ does not depend on the number of conjugations q. Based on the above, we select the magnitudes of the eighth-order CCs with q even to identify ASK, PSK, and QAM signals.[1] The delay vectors and CFs at which we calculate these CC magnitudes have to be chosen to completely define the discriminating signal features. Spooner introduced an ideal classifier, with features based on the CCs of all orders n, computed at all delay vectors and CFs; however, due to the impossibility of implementation, an order-, delay- and CF-reduced classifier needs to be developed [11]. Here we consider the zero-delay vector for simplicity of estimation (see Appendix "1" for the sample estimate of the nth order/q-conjugate CCs), and frequency $\beta = 1/\rho$. A CC-based feature vector is formed to be used for modulation recognition, as

$$\mathbf{F}^{(i)} = [|c_y^{(i)}(\gamma_0; \mathbf{0}_8)_{8,0}||c_y^{(i)}(\gamma_2; \mathbf{0}_8)_{8,2}||c_y^{(i)}(\gamma_4; \mathbf{0}_8)_{8,4}||c_y^{(i)}(\gamma_6; \mathbf{0}_8)_{8,6}||c_y^{(i)}(\gamma_8; \mathbf{0}_8)_{8,8}|]^{\dagger}, \quad i = 1, \ldots, N_{\text{mod}}, \tag{10}$$

where the CFs $\gamma_q, q = 0, 2, 4, 6, 8$, are given by (3) and (7), with $\beta = 1/\rho, n = 8$, and corresponding q. The features can be calculated according to (9), by using the values of the cumulants of the modulations of interest given in Table 1 and estimates of the signal amplitude and pulse shape. An estimate of the feature vector is obtained based on N observed symbols, $\hat{\mathbf{F}}_N$, by replacing ensemble averages by sample average. For simplicity, the Euclidian norm is used as a distance metric, and the decision criterion is

$$\text{Choose the modulation format } \bar{i} \text{ if } \bar{i} = \arg \min_{1 \leq i \leq N_{\text{mod}}} ||\hat{\mathbf{F}}_N - \mathbf{F}^{(i)}||_2. \tag{11}$$

4 Multi-Antenna Cyclic Cumulant-Based Classifier in Fading Channels

In this section, a multi-antenna modulation classifier, which employs eighth-order CC-based features, is proposed. The multi-antenna classifier takes advantage of spatial diversity by combining several independent copies of the signal to combat fading. To combine the signals received by multiple antennas, before the modulation recognition, a selection combiner [24,25] is chosen, as it does not need channel estimates. An L branch receive antenna array is considered, with fading amplitudes and phases among the L diversity channels independent. Furthermore, the L noise processes are assumed independent zero-mean complex Gaussians, with identical autocorrelation functions. The L sampled signals, $y_\ell^{(i)}(m)$, $\ell = 1, 2, \ldots, L$, are applied to a selection combiner, where the branch yielding the highest instantaneous signal-to-noise ratio (SNR) is selected. The discrete-time signal at the output of the diversity combiner is therefore given by

[1] In addition to the signals given in Table 1, these features can be used to identify other modulations, e.g., 128-QAM, 256-QAM, V29, etc. If M-PSK modulations with $M > 16$ are included in the pool, the proposed eighth-order CC-based features can be used to decide whether the modulation of the incoming signal is either M-PSK, $M \geq 16$, or one of the 4-ASK, 8-ASK, BPSK, QPSK, 8-PSK, 16-QAM, 32-QAM, and 64-QAM signals.

$$y_{SC}^{(i)}(m) = y_{\ell'}^{(i)}(m), \quad \ell' = \underset{1 \le \ell \le L}{\arg\max}\ \eta_\ell, \tag{12}$$

where η_ℓ is the received instantaneous SNR of the ℓ-th branch [24]. Apparently, the nth-order/q-conjugate CCs of the sampled signal at the output of the selection combiner are given by (8), with ℓ replaced by ℓ', defined in (12). With the proposed multi-antenna classifier, MC is performed as described in Sect. 3 for the single-antenna classifier, by processing the signal at the output of the selection combiner.

5 Simulation Results and Discussion

5.1 Simulation Setup

With $N_{\text{mod}} = 9$, the pool of modulation consists of 4-ASK, 8-ASK, BPSK, QPSK, 8-PSK, 16-PSK, 16-QAM, 32-QAM, and 64-QAM. Normalized modulations are simulated, i.e., $E[|s_k^{(i)}|^2] = 1, i = 1, \ldots, N_{\text{mod}}$. The transmit and receive filters are square-root raised cosine pulses with $r = 0.35$ roll-off factor, simulated as finite-impulse response (FIR) filters with $(16\rho + 1)$ taps. Hence, the length of each FIR impulse response is $(16\rho + 1)T/\rho = 16T + T/\rho$ sec. The oversampling factor ρ is chosen to be 11, to eliminate aliasing in both cycle and spectral frequency domains (see the results in Appendix "3" for $n = 8$ and $r = 0.35$). In all simulations we set $T = 1, \varepsilon = 0.7$, and $\Delta f = 0$. For each branch, the noise sequence at the output of the receive filter was generated by passing a zero-mean white Gaussian sequence with autocorrelation $\sigma_w^2 \delta(\tau_d)$ through the square-root raised cosine receive filter, where σ_w^2 is the noise power and $\delta(.)$ is the Dirac delta function. Furthermore, the channel coefficients are generated as identical distributed complex Gaussians, such that the fading power equals one. The average (per-branch) SNR, calculated at the output of the receive filter, is used in simulations. The number of processed symbols, N, is equal to 4,000, unless otherwise mentioned. Perfect estimates of the amplitude, frequency offset, and pulse shape are assumed.

In classifying N_{mod} equiprobable modulations, the average probability of correct classification, $P_{cc} = N_{\text{mod}}^{-1} \sum_{i=1}^{N_{\text{mod}}} P_c^{(i|i)}$, is used to quantify the classification performance, with the probability of correct classification for modulation i, $P_c^{(i|i)}$, $i = 1, \ldots, N_{\text{mod}}$, estimated based on 300 Monte Carlo trials.

5.2 Single- and Multi-Antenna CC-Based Classifiers in Rayleigh Fading

In Fig. 1 the average probability of correct classification, P_{cc}, for $L = 1, 2$, and 4 is plotted versus the average SNR per branch. One can easily notice that by adding only the second antenna, we obtain a large performance improvement when compared with the single-antenna classifier.

5.3 Effect of the Number of Antennas

In Fig. 2 the effect of L on the number of symbols required to achieve a certain P_{cc} is shown. Results are obtained for 15 dB average SNR per branch. As one can easily notice from Fig. 2, a smaller number of symbols is needed to attain a specific performance when using the diversity combiner. For example, $P_{cc} = 0.9$ is obtained with 1,900 and 2,300 symbols, when

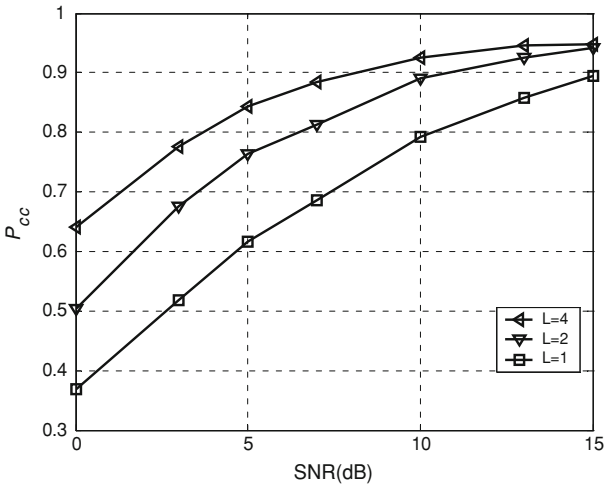

Fig. 1 Performance versus SNR in Rayleigh fading, for different number of branches and $N = 4{,}000$ symbols

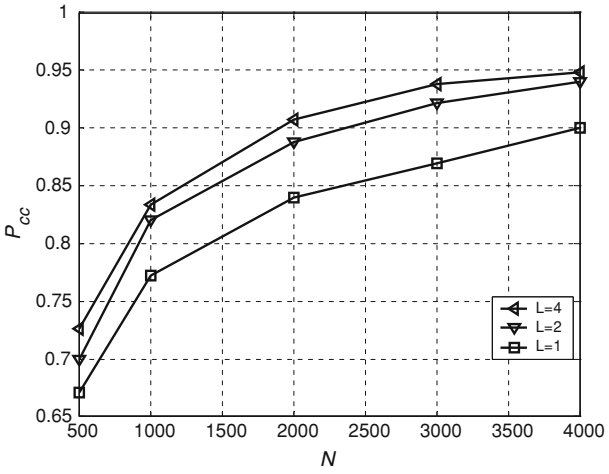

Fig. 2 Performance versus the number of symbols N in Rayleigh fading, for different number of branches and SNR = 15 dB

using four and two antennas, respectively, whereas with a single antenna, 4,000 symbols are required for the same performance.

5.4 Effect of the Spatial Correlation Among the Branches

So far we have assumed negligible correlation among branches. To examine the impact of correlation on the performance, we consider two correlated Rayleigh fading branches, with the correlation defined by $\varsigma_{12} = \mathrm{E}\left[\mu_1 \mu_2^*\right]$, where $\mu_1 = \alpha_1 e^{j\varphi_1}$ and $\mu_2 = \alpha_2 e^{j\varphi_2}$ are zero-mean dependent complex Gaussian variables. For the two correlated branches, simulated such that $0 \leq \varsigma_{12} \leq 1$, the performance shown in Fig. 3 is better at higher average SNRs per branch, degrades at very high correlations, and appears to be robust to correlations as large as 0.8.

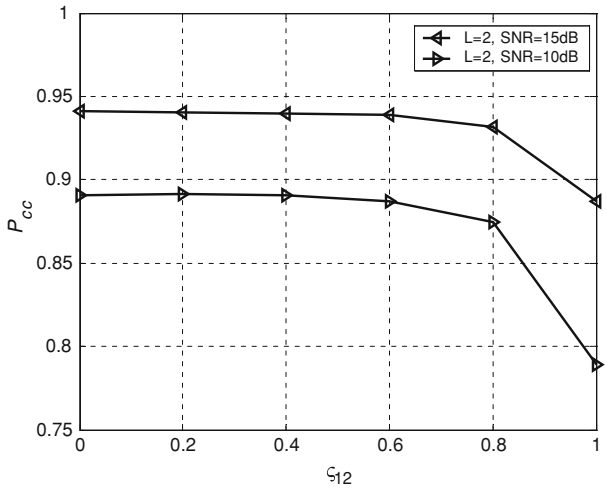

Fig. 3 Performance of a two branch classifier in Rayleigh fading versus the correlation among branches, for $N = 4{,}000$ symbols and different SNRs

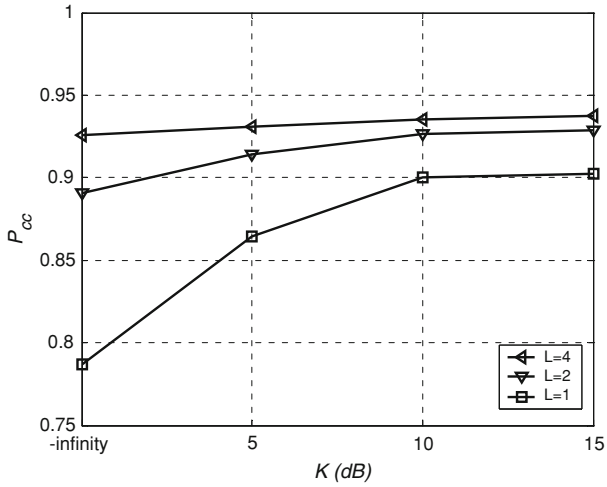

Fig. 4 Performance versus the Rice factor in Rice fading, for different number of branches, $N = 4{,}000$ symbols, and SNR = 10 dB

5.5 Effect of the K Factor in Rice Fading

Performance of the multi-antenna CC classifier in Rice fading is shown in Fig. 4, versus the Rice K factor,[2] at 10 dB average SNR per branch. Notice the significant performance enhancement, obtained by adding only one extra antenna, i.e., $L = 2$ compared with $L = 1$, at low values of K. As expected, the classifier performance improves with K, from $K = 0$ (Rayleigh fading) to $K = \infty$ (no fading). Also note that with $L > 1$, the classifier performance is robust to the variations of the K factor.

[2] For the definition of the Rice K factor see, for example, [25] Chap. 1.

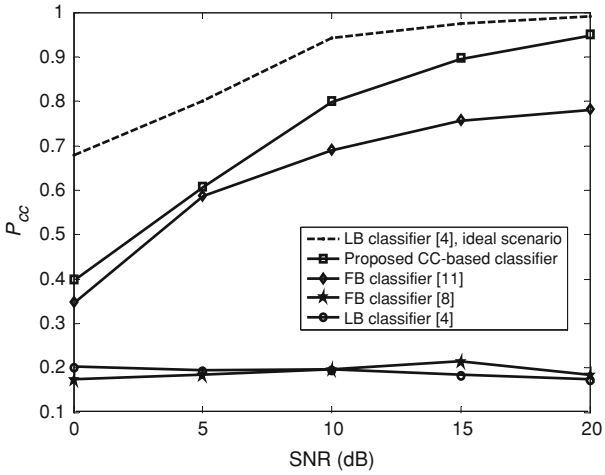

Fig. 5 Performance comparison of different single-antenna classifiers, for $N = 4{,}000$ symbols

5.6 Performance Comparison of the Proposed Single-Antenna CC-Based Classifier with LB and Other FB Classifiers

Performance of the proposed single-antenna CC-based classifier is compared against that of classifiers introduced in [4,8], and [11], when recognizing BPSK, QPSK, 8-PSK, 16-PSK, 16-QAM, and 64-QAM modulations in Rayleigh fading ($N_{\text{mod}} = 6$). Unless otherwise mentioned, parameters are set up as per Sect. 5.1. Note that classifiers in [4,8], and [11] are single-antenna, as well. Furthermore, a raised cosine pulse shape is considered with these classifiers and the SNR is defined at the output of receive-filter to ensure a fair comparison. An LB classifier is proposed in [4], whereas FB classifiers in [8] and [11]. The LB classifier in [4] assumes known parameters. The classifier in [8] employs the magnitude of the normalized fourth-order/ zero-conjugate cumulant as discriminating feature, with normalization to the second power of the second-order/ one-conjugate cumulant of the signal component, and is robust to phase. The classifier in [11] uses a feature vector whose components are the magnitudes of the nth-order/ q-conjugate CCs raised to the power of $1/n$, $n = 2, 4, 6$, $q = 0, \ldots, n$, and is robust to phase and timing offset. It is noteworthy that by using statistics with order lower than eight, the FB classifiers in [8] and [11] cannot distinguish between 8-PSK and 16-PSK. Results obtained with the aforementioned classifiers are presented in Fig. 5, and show that the proposed CC-based classifier outperforms classifiers in [4,8], and [11]. Moreover, the classifiers in [4] and [8] fail under the investigated scenario, as they are not robust to phase and timing offset, and timing offset, respectively. Results achieved with the LB classifier when assuming known parameters is also presented, as representing the maximum performance (ideal scenario). As one can easily notice, the proposed classifier provides a reasonable performance under the investigated non-ideal scenario at higher SNRs, e.g., a P_{cc} above 0.8 is attained for SNRs above 10 dB.

6 Conclusion

In this correspondence we have introduced single- and multi-antenna higher-order cyclic cumulant-based classifiers for linear digital modulations in flat fading channels. The proposed

single-antenna classifier has the advantage of robustness to unknown phase and timing offset, being applicable to a large pool of modulations. Furthermore, the multi-antenna classifier mitigates the impact of fading by employing selection combining as a spatial diversity scheme. This is also shown to be robust to a possible correlation among the antennas, as well as the variations of the Rice K factor, which represents different levels of fading. A fair comparison with other classifiers proposed in the literature is performed, proving the effectiveness of the proposed classifier. In addition, analytical closed-form expressions for the higher-order cyclic cumulant polyspectra have been derived for linearly digitally modulated signals affected by fading channel, frequency and timing offsets, and additive Gaussian noise. For a raised cosine pulse shape, a necessary and sufficient condition for the oversampling factor is obtained to avoid aliasing in the cycle and spectral frequency domains.

Acknowledgment Octavia A. Dobre would like to thank Dr. C. M. Spooner for the useful discussions on signal cyclostationarity.

Appendix 1: Cumulants, Cyclic Cumulants, and Sample Estimates

For a complex-valued continuous-time nth-order cyclostationary process, $y^{(i)}(t)$, the nth-order/ q-conjugate time-varying cumulant, $\tilde{c}_y^{(i)}(t;\tilde{\boldsymbol{\tau}})_{n,q}$, is an (almost) periodic function of time, and can be expressed as an exponential Fourier series [20,21],[3]

$$\tilde{c}_y(t,\tilde{\boldsymbol{\tau}})_{n,q} = \sum_{\tilde{\gamma}\in\tilde{\kappa}_{n,q}} \tilde{c}_y(\tilde{\gamma};\tilde{\boldsymbol{\tau}})_{n,q} e^{j2\pi\tilde{\gamma}t}, \tag{13}$$

where the coefficient represents the nth-order/q-conjugate CC of $y^{(i)}(t)$ at cycle frequency $\tilde{\gamma}$ and delay vector $\tilde{\boldsymbol{\tau}}$, given by

$$\tilde{c}_y^{(i)}(\tilde{\gamma};\tilde{\boldsymbol{\tau}})_{n,q} = \lim_{I\to\infty} I^{-1}\int_{-I/2}^{I/2} \tilde{c}_y^{(i)}(t;\tilde{\boldsymbol{\tau}})_{n,q} e^{-j2\pi\tilde{\gamma}} dt.$$

The nth-order/ q-conjugate time-varying cumulant is expressed in terms of the nth- and lower-orders moments, through the moment to cumulant formula, as [20,21][3]

$$\begin{aligned}\tilde{c}_y^{(i)}(t;\tilde{\boldsymbol{\tau}})_{n,q} &= \mathrm{Cum}[y^{(i)^{(*)_1}}(t+\tilde{\tau}_1)\ldots y^{(i)^{(*)_{n-1}}}(t+\tilde{\tau}_{n-1})y^{(i)^{(*)_n}}(t)] \\ &= \sum_{\{\wp_1,\ldots,\wp_Z\}} (-1)^{Z-1}(Z-1)!\prod_{z=1}^{Z}\tilde{m}_y^{(i)}(t;\tilde{\boldsymbol{\tau}}_z)_{n_z,q_z},\end{aligned} \tag{14}$$

where $(*)_u$, $u=1,\ldots,n$, represents a possible conjugation, so that the total number of conjugations is q, $\{\wp_1,\ldots,\wp_Z\}$ is a partition of $\wp=\{1,2,\ldots,n\}$, with $\wp_z$'s, $z=1,\ldots,Z$, as non-empty disjoint subsets of $\wp$, so that their reunion is $\wp$, Z is the number of the subsets in a partition ($1\le Z\le n$), $\tilde{\tau}_z$ is a delay vector whose components are elements of $\{\tilde{\tau}_1,\ldots,\tilde{\tau}_{n-1},\tilde{\tau}_n=0\}$, with indices specified by $\wp_z$, and n_z is the number of elements in the subset $\wp_z$, from which q_z correspond to conjugate terms. Note that $\sum_{z=1}^{Z} n_z = n$ and $\sum_{z=1}^{Z} q_z = q$. Furthermore, $\tilde{m}_y^{(i)}(t;\tilde{\boldsymbol{\tau}}_z)_{n_z,q_z}$ is the n_zth-order/q_z conjugate time-varying moment of $y^{(i)}(t)$, defined as

$$\tilde{m}_y^{(i)}(t;\tilde{\boldsymbol{\tau}}_z)_{n_z,q_z} = \mathrm{E}[y^{(i)^{(*)_{1,z}}}(t+\tilde{\tau}_{1,z})y^{(i)^{(*)_{1,z}}}(t+\tilde{\tau}_{1,z})\ldots y^{(i)^{(*)_{n,z}}}(t+\tilde{\tau}_{n,z})], \tag{15}$$

[3] In [20,21] the definitions of time-domain parameters of higher-order cyclostationary are given for real processes. As complex processes are encountered in MC, here we extend the definitions to this case.

where $\tilde{\tau}_{v,z}, v = 1, \ldots, n_z$, are the components of the delay vector $\tilde{\tau}_z$, and $(*)_{v,z}, v = 1, \ldots, n_z$, represents a possible conjugation, corresponding to the subset $\wp_z$ and the conjugate terms in (14), so that the total number of conjugations is q_z.

The nth-order/q-conjugate CC of $y^{(i)}(t)$ at cycle frequency $\tilde{\gamma}$ and delay vector $\tilde{\boldsymbol{\tau}}$ can be expressed as [20,21][3]

$$\tilde{c}_y^{(i)}(\tilde{\gamma}; \tilde{\boldsymbol{\tau}})_{n,q} = \sum_{\{\wp_1, \ldots, \wp_Z\}} (-1)^{Z-1}(Z-1)! \sum_{\tilde{\boldsymbol{\chi}}^\dagger 1 = \tilde{\gamma}} \prod_{z=1}^{Z} \tilde{m}_y^{(i)}(\tilde{\chi}_z; \tilde{\boldsymbol{\tau}}_z)_{n_z,q_z}, \tag{16}$$

where $\tilde{\boldsymbol{\chi}} = [\tilde{\chi}_1, \ldots, \tilde{\chi}_Z]^\dagger$ is a vector of CFs, 1 is a Z-dimensional one vector, and $\tilde{m}_y^{(i)}(\tilde{\chi}_z; \tilde{\boldsymbol{\tau}}_z)_{n_z,q_z}$ is the n_z th-order/q_z-conjugate cyclic moment of $y^{(i)}(t)$ at cycle frequency $\tilde{\chi}_z$ and delay vector $\tilde{\tau}_z$, defined as[3]

$$\tilde{m}_y^{(i)}(\tilde{\chi}_z; \tilde{\boldsymbol{\tau}}_z)_{n_z,q_z} = \lim_{I \to \infty} I^{-1} \int_{-I/2}^{I/2} \tilde{m}_y^{(i)}(t; \tilde{\boldsymbol{\tau}}_z)_{n_z,q_z} e^{-j2\pi \tilde{\chi}_z t} dt. \tag{17}$$

Equation (16) represents the so called cyclic moment to cumulant formula, which gives the nth-order CCs as a function of the nth- and lower-orders cyclic moments. The nth-order/q-conjugate CCs of the discrete-time signal $y^{(i)}(m) = y^{(i)}(t)\big|_{t=mT/\rho}$ is given by (5). A similar expression can be also written for cyclic moments [23]. Furthermore, (13)–(17) can be easily rewritten for discrete-time signals (see, for example, [26]). The estimate of the n_zth-order/q_z-conjugate cyclic moment based on N observed symbols ($N\rho$ samples) is given by [26]

$$\begin{aligned}\hat{m}_y^{(i)}(\chi_z; \boldsymbol{\tau}_z)_{n_z,q_z} = (N\rho)^{-1} \sum_{m=1}^{N\rho} & y^{(i)^{(*)_{1,z}}}(m + \tau_{1,z}) y^{(i)^{(*)_{2,z}}}(m + \tau_{2,z}) \ldots \\ & \times y^{(i)^{(*)_{n_z,z}}}(m + \tau_{n_z,z}) e^{-j2\pi \chi_z m},\end{aligned} \tag{18}$$

where $\boldsymbol{\tau}_z = \tilde{\boldsymbol{\tau}}_z \rho / T$, with its components $\tau_{v,z} = \tilde{\tau}_{v,z}\rho/T, v = 1, \ldots, n_z$, and $\chi_z = \tilde{\chi}_z T/\rho$. Then, the estimate of the nth-order/q-conjugate CCs, based on N observed symbols, $\hat{c}_y^{(i)}(\gamma; \boldsymbol{\tau})_{n,q}$, is obtained by replacing the cyclic moment estimates in the cyclic moment to cumulant formula [26].

Equations (14)–(15) can be easily written for stationary processes, by dropping the t-dependency, and further simplified for random variables [19]. Let us consider the variable $s_k^{(i)}$, with values taken from the alphabet corresponding to the i-th signal constellation, $i = 1, \ldots, N_{\text{mod}}$. The n_zth-order/q_z-conjugate moment of the i-th constellation is defined as

$$m_{s^{(i)},n_z,q_z} = \mathrm{E}[(s_k^{(i)^*})^{q_z}(s_k^{(i)})^{n_z - q_z}] = M_i^{-1} \sum_{m=1}^{M_i} (s_m^{(i)^*})^{q_z}(s_m^{(i)})^{n_z - q_z}. \tag{19}$$

Then, by using the moment to cumulant formula, the nth-order/q-conjugate cumulant of the i-th constellation, $c_{s^{(i)},n,q}$, can be easily expressed in terms of moments as

$$\begin{aligned} c_{s^{(i)},n,q} &= \mathrm{Cum}[(s_k^{(i)^*})^q (s_k^{(i)})^{n-q}] \\ &= \sum_{\{\wp_1, \ldots, \wp_Z\}} (-1)^{Z-1}(Z-1)! \prod_{z=1}^{Z} m_{s^{(i)},n_z,q_z}. \end{aligned} \tag{20}$$

Appendix 2: Derivation of the Analytical Closed-Form Expressions for Higher-Order Cyclic Cumulants and Cycle Frequencies

With the signal model in (1), and by using the cumulant properties [19], one can easily show that the nth-order/q-conjugate time-varying cumulant of $y^{(i)}(t)$ at delay vector $\tilde{\tau}$ is given by (note that the conjugated terms are arbitrarily chosen)

$$\begin{aligned}\tilde{c}_y^{(i)}(t;\tilde{\boldsymbol{\tau}})_{n,q} &= \mathrm{Cum}[y^{(i)*}(t+\tilde{\tau}_1)\ldots y^{(i)*}(t+\tilde{\tau}_q)y^{(i)}(t+\tilde{\tau}_{q+1})\ldots y^{(i)}(t)]\\ &= \alpha^n e^{j\varphi(n-2q)} e^{j2\pi\Delta f(-\tilde{\tau}_1-\cdots-\tilde{\tau}_q+\tilde{\tau}_{q+1}+\cdots+\tilde{\tau}_{n-1})} e^{j2\pi(n-2q)\Delta f t}\\ &\quad\times \sum_{k_1}\sum_{k_2}\cdots\sum_{k_n}\mathrm{Cum}[s^*_{k_1+\xi_1},\ldots,s^*_{k_q+\xi_q},s_{k_{q+1}+\xi_{q+1}},\ldots,s_{k_n}]\\ &\quad\times p^*(t-k_1T-\varepsilon T+\tilde{\tau}_1)\ldots\\ &\quad\times p^*(t-k_qT-\varepsilon T+\tilde{\tau}_q)p(t-k_{q+1}T-\varepsilon T+\tilde{\tau}_{q+1})\ldots p(t-k_nT-\varepsilon T).\end{aligned} \tag{21}$$

The notation $s^{(i)}_{k_u+\xi_u}=s^{(i)}(k_uT+\xi_uT)$ used in (21), in which $\xi_uT=\tilde{\tau}_u$, $u=1,\ldots,n-1$, with ξ_u not necessarily an integer, shows that delayed versions of the symbol transmitted within the k_uth period need to be considered. Under the assumption of independent data symbols, the cumulant $\mathrm{Cum}[s^*_{k_1+\xi_1}\ldots s^*_{k_q+\xi_q}s_{k_{q+1}+\xi_{q+1}}\ldots s_{k_n}]$ is non-zero if and only if $s^{(i)}_{k_1+\xi_1}=\ldots=s^{(i)}_{k_n}$, which occurs for $k_1=\ldots=k_n=k$ and delays $\tilde{\tau}_u$, $u=1,\ldots,n-1$, depending on the pulse shape. For example, these delays belong to the interval $[0,T)$ for a rectangular pulse shape, and exceed T for a raised cosine pulse shape. In such case $\mathrm{Cum}[s^*_{k_1+\xi_1}\ldots s^*_{k_q+\xi_q}s_{k_{q+1}+\xi_{q+1}}\ldots s_{k_n}]=c_{s^{(i)},n,q}$, and (21) can be further written as

$$\begin{aligned}\tilde{c}_y^{(i)}(t;\tilde{\boldsymbol{\tau}})_{n,q} &= \alpha^n c_{s^{(i)},n,q} e^{j\varphi(n-2q)} e^{j2\pi\Delta f\sum_{u=1}^{n-1}(-)_u\tilde{\tau}_u} e^{j2\pi(n-2q)\Delta f t}\\ &\quad\times\prod_{u=1}^{n-1}p^{(*)_u}(t+\tilde{\tau}_u)p^{(*)_n}(t)\otimes\sum_k\delta(t-kT-\varepsilon T),\end{aligned} \tag{22}$$

where $\otimes$ denotes the convolution operator.

By applying the Fourier transform to (22) with respect to t, and after some mathematical manipulations, one can show that

$$\begin{aligned}\Im\{\tilde{c}_y^{(i)}(t;\tilde{\boldsymbol{\tau}})_{n,q}\} &= \alpha^n c_{s^{(i)},n,q}T^{-1}e^{j\varphi(n-2q)}e^{j2\pi\Delta f\sum_{u=1}^{n-1}(-)_u\tilde{\tau}_u}e^{-j2\pi\tilde{\beta}\varepsilon T}\\ &\quad\times\sum_k\int_{-\infty}^{\infty}\prod_{u=1}^{n-1}p^{(*)_u}(t+\tilde{\tau}_u)p^{(*)_n}(t)e^{-j2\pi tkT^{-1}}dt\\ &\quad\times\delta\left(\tilde{\gamma}-kT^{-1}-(n-2q)\Delta f\right),\end{aligned} \tag{23}$$

where $\Im\{.\}$ denotes the Fourier transform. It is straightforward that (23) represents a sum of spectral components at frequencies $\{\tilde{\gamma}\}$ specified in (3), and with coefficients given in (2). In other words, the nth-order/q-conjugate time-varying cumulant can be expressed as a sum of complex exponentials with frequencies corresponding to the CFs, and the nth-order/q-conjugate CCs as coefficients. It should be noted that results presented in [20,21] represent a particular case of (2) and (3), for $\varepsilon=0$, $\Delta f=0$, $\alpha=1$, and $\varphi=0$. In addition, results presented in (2) and (3) are also given in [10], but with no proof.

Appendix 3: Simple Examples of Cyclic Cumulants and Cycle Frequencies

The nth-order/q-conjugate CCs of $y^{(i)}(t)$ in (1) and the set of associated CFs are given by (2) and (3), respectively. For a better understanding, here we provide two examples: $(n, q) = (4, 0)$ and (4,2). For $(n, q) = (4, 0)$, (2) and (3) simplify, respectively, to

$$\tilde{c}_y^{(i)}(\tilde{\gamma};\tilde{\boldsymbol{\tau}})_{4,0} = \alpha^4 c_{s^{(i)},4,0} T^{-1} e^{-j2\pi\tilde{\beta}\varepsilon T} e^{j4\varphi} e^{j2\pi\Delta f(\tilde{\tau}_1+\tilde{\tau}_2+\tilde{\tau}_3)} \times \int_{-\infty}^{\infty} p(t)p(t+\tilde{\tau}_1)p(t+\tilde{\tau}_2)p(t+\tilde{\tau}_3)e^{-j2\pi t\tilde{\beta}}dt, \tag{24}$$

$$\tilde{\kappa}_{4,0} = \{\tilde{\gamma} : \tilde{\gamma} = \tilde{\beta} + 4\Delta f, \tilde{\beta} = k/T, k \text{ integer}, \tilde{c}_y^{(i)}(\tilde{\gamma};\tilde{\boldsymbol{\tau}})_{4,0} \neq 0\}, \tag{25}$$

whereas for $(n, q) = (4, 2)$ we obtain

$$\tilde{c}_y^{(i)}(\tilde{\gamma};\tilde{\boldsymbol{\tau}})_{4,2} = \alpha^4 c_{s^{(i)},4,2} T^{-1} e^{-j2\pi\tilde{\beta}\varepsilon T} e^{j2\pi\Delta f(\tilde{\tau}_1+\tilde{\tau}_2-\tilde{\tau}_3)} \times \int_{-\infty}^{\infty} p^*(t)p(t+\tilde{\tau}_1)p(t+\tilde{\tau}_2)p^*(t+\tilde{\tau}_3)e^{-j2\pi t\tilde{\beta}}dt, \tag{26}$$

$$\tilde{\kappa}_{4,2} = \{\tilde{\gamma} : \tilde{\gamma} = \tilde{\beta}, \tilde{\beta} = k/T, k \text{ integer}, \tilde{c}_y^{(i)}(\tilde{\gamma};\widehat{\boldsymbol{\tau}})_{4,2} \neq 0\}. \tag{27}$$

The elements of the cycle frequency sets, k's, are explicitly given in Appendix "5" for a raised cosine pulse shape. Note that in (26) the first and fourth p terms are conjugated. However, we can choose any other pair in that product to conjugate. Anyway, as long as $p(t)$ is real, which is the case in this correspondence, this is not an issue.

Appendix 4: Derivation of the Analytical Closed-Form Expression for the Higher-Order Cyclic Cumulant Polyspectra

By taking the $(n-1)$ fold Fourier transform of $\tilde{c}_y^{(i)}(\tilde{\gamma};\tilde{\tau})_{n,q}$ given in (2) with respect to $\tilde{\tau} = [\tilde{\tau}_1 \ldots \tilde{\tau}_{n-1}]^{\dagger}$, one can easily write that

$$\tilde{C}_y^{(i)}(\tilde{\gamma};\tilde{\mathbf{f}})_{n,q} = \alpha^n c_{s^{(i)},n,q} T^{-1} e^{-j2\pi\tilde{\beta}\varepsilon T} e^{j(n-2q)\varphi} \times \int_{-\infty}^{\infty} p^{(*)_n}(t) e^{-j2\pi\tilde{\beta}t} \prod_{u=1}^{n-1} \int_{-\infty}^{\infty} p^{(*)_u}(t+\tilde{\tau}_u) e^{j2\pi\Delta f \sum_{u=1}^{n-1}(-)_u\tau_u} e^{j2\pi\tilde{f}_u\tilde{\tau}_u} d\tilde{\tau}_u dt. \tag{28}$$

With the change of variable $\tilde{v}_1 = t + \tilde{\tau}_1, \ldots, \tilde{v}_{n-1} = t + \tilde{\tau}_{n-1}, \tilde{v}_n = t$, and after simple mathematical manipulations, one can easily find the expression for the nth-order/q-conjugate CCPs of $y^{(i)}(t)$ in (4). It should be noted that results presented in [20,21] represent a particular case of (4), for $\varepsilon = 0$, $\Delta f = 0$, $\alpha = 1$, and $\varphi = 0$.

Appendix 5: The Set of Cycle Frequencies and a Proper Selection of the Oversampling Factor

Here we derive the set $\tilde{\kappa}_{n,q}$ of CFs for a raised cosine pulse shape, as a function of the roll-off factor, r. To illustrate the procedure, we start with an example for $n = 4$ and $q = 2$. In such case (4) becomes

$$\tilde{C}_y^{(i)}(\tilde{\gamma};[\tilde{f}_1,\tilde{f}_2,\tilde{f}_3])_{4,2} = \alpha^4 c_{s^{(i)},4,2} T^{-1} e^{-j2\pi\tilde{\beta}\varepsilon T} \times P^*(-\tilde{\beta}+\tilde{f}_1-\Delta f+\tilde{f}_2-\Delta f-(-\tilde{f}_3-\Delta f)) \times P(\tilde{f}_1-\Delta f)P(\tilde{f}_2-\Delta f)P^*(-\tilde{f}_3-\Delta f), \quad (29)$$

where the two conjugated terms are arbitrarily chosen in the product given in (29).

$$\tilde{C}_y^{(i)}(\tilde{\gamma};[\tilde{f}_1,\tilde{f}_2,\tilde{f}_3])_{4,2} \neq 0 \quad \text{if} \begin{cases} c_{s^{(i)},4,2} \neq 0 \quad \text{and,} \\ P(\tilde{f}_1-\Delta f)\neq 0,\ P(\tilde{f}_2-\Delta f)\neq 0,\ P^*(-\tilde{f}_3-\Delta f)\neq 0 \quad \text{and,} \\ P^*(-\tilde{\beta}+\tilde{f}_1-\Delta f+\tilde{f}_2-\Delta f-(-\tilde{f}_3-\Delta f))\neq 0. \end{cases} \quad (30)$$

With a raised cosine pulse shape bandlimited to $B_p = (1+r)/(2T)$, the conditions imposed in (30) yield $|\tilde{f}_1 - \Delta f| < B_p$ (C.1), $|\tilde{f}_2 - \Delta f| < B_p$ (C.2), $|-\tilde{f}_3 - \Delta f| < B_p$ (C.3) and $|-\tilde{\beta}+\tilde{f}_1-\Delta f+\tilde{f}_2-\Delta f-(-\tilde{f}_3-\Delta f)| < B_p$ (C.4). Hence, a necessary condition for $\tilde{\beta}$ is $|\tilde{\beta}| < 4B_p$. By replacing $\tilde{\beta} = k/T$ and $B_p = (1+r)/(2T)$ in the above inequality, the following results can be easily obtained: the set $\{\tilde{\beta}\}_4$ is given by $\{0, \pm 1/T\}$ if $r = 0$, $\{0, \pm 1/T, \pm 2/T\}$ if $0 < r \leq 0.5$ and $\{0, \pm 1/T, \pm 2/T, \pm 3/T\}$ if $0.5 < r \leq 1$. One can show that if $c_{s^{(i)},4,q} \neq 0$, the same result holds for $n = 4$, with $q = 0, 1, 3$ or 4. Otherwise, $\tilde{\kappa}_{4,q}$ is the null set.

The same procedure can be applied for any n and q. If n is odd, the set of CFs is the null set, since for the signal of interest $c_{s^{(i)},n,q} = 0$, for any $q = 0, \ldots, n$. With n even, the following results can be easily obtained. First, $|\tilde{\beta}| < nB_p$ is a necessary condition for $\tilde{\beta}$, any n and $q = 0, \ldots, n$. Then, the set $\{\tilde{\beta}\}_n$ is given by $\{0, \ldots, \pm(n/2-1)/T\}$ if $r = 0$, and includes $\{0, \ldots, \pm n/(2T)\}$ if $0 < r \leq 1$. Additional values for $\tilde{\beta}$ can exist in different r regions. By mathematical induction it can be easily proved that if $2m/n < r \leq (2m+2)/n$, $m = 1, \ldots, n/2-1$, the set of additional values for $\tilde{\beta}$ is $\{\pm(n+2)/(2T), \ldots, \pm(n+2m)/(2T)\}$. Once the set $\{\tilde{\beta}\}_n$ is determined, the set $\kappa_{n,q}$ of CFs is computed using (3). Results presented in [27] can be seen as particular cases of these findings.

By knowing the set $\{\tilde{\beta}\}_n$, a necessary and sufficient condition for the oversampling factor ρ to eliminate aliasing can be derived for any n and r. The nth-order CCPs of the sampled signal at the output of the receive filter is given by [23]

$$C_y^{(i)}(\gamma;\mathbf{f})_{n,q} = f_s^{n-1} \sum_{v\in Z} \sum_{\boldsymbol{\nu}\in Z^{n-1}} \tilde{C}_y^{(i)}(\tilde{\gamma}-vf_s;\tilde{\mathbf{f}}-\boldsymbol{\nu}f_s)_{n,q}, \quad (31)$$

with f_s as the sampling frequency, $\gamma = \tilde{\gamma}/f_s$, $\mathbf{f} = \tilde{\mathbf{f}}/f_s$, Z the set of all integers, and $\boldsymbol{\nu} = [\nu_1, \ldots, \nu_{n-1}]^\dagger$, where each ν_u, $u = 1, \ldots, n-1$, is an integer. One can notice that the nth-order CCPs of the sampled signal consist of the periodic extension of the nth-order CCPs of the original continuous signal, in both spectral ($\tilde{\mathbf{f}} - \boldsymbol{\nu}f_s$) and cycle frequency ($\tilde{\gamma} - vf_s$) domains. Two kinds of aliasing effects can appear due to sampling, i.e., aliasing in the spectral frequency domain, which is the overlapping of images of CCP with the same cycle frequency, and aliasing in the cycle frequency domain, which is the overlapping of images of the CCP with different cycle frequencies. Let us consider $n = 4$ and $q = 2$. Obviously, based on (C.1)–(C.3), the Nyquist condition needs to be fulfilled to eliminate aliasing in the spectral frequency domain. This translates into the condition $\rho \geq r + 1$ for the oversampling factor. It can be easily shown that this holds for any and n and q. Let us further assume that $r = 1$. In such case, as for the examined signals $c_{s^{(i)},4,2} \neq 0$ (see Table 1), the set $\tilde{\kappa}_{4,2}$ of CFs is $\{0, \pm 1/T, \pm 2/T, \pm 3/T\}$. By using this result and (31), it is apparent that the sampling frequency f_s needs to be at least $7/T$ to avoid aliasing in the cycle frequency domain. This

translates into a condition for the oversampling factor ρ, which has to be at least 7. Based on the previously derived set of frequencies $\{\tilde{\beta}\}_n$, n even, it is straightforward that if $c_{s^{(i)},n,q} \neq 0$, the condition for the sampling frequency f_s to avoid cycle aliasing is to be at least $(n-1)/T$ for $r = 0$ and $(n+2m+1)/T$ for $2m/n < r \leq (2m+2)/n, m = 0, \ldots, n/2-1$, which respectively translate into the conditions $\rho \geq n-1$ and $\rho \geq n+2m+1$ for the oversampling factor. Furthermore, it can be easily shown that in such case spectral aliasing is also avoided if these conditions are fulfilled.

References

1. Haykin, S. (2005). Cognitive radio: Brain-empowered wireless communications. *IEEE Journal on Selected Areas in Communications, 23*, 201–220.
2. Kyouwoong, K., Akbar, I. A., Bae, K., Um, J.-S., Spooner, C. M., & Reed, J. (2007). Cyclostationary approach to signal detection and classification in cognitive radio. In *Proceedings of IEEE DySPAN* (pp. 212–215).
3. Dobre , O. A., Abdi, A., Bar-Ness, Y., & Su, W. (2007). A survey of automatic modulation classification techniques: Classical approaches and new trends. *IET Processing Communications, 1*(2), 137–156.
4. Wei, W., & Mendel, J. M. (2000). Maximum-likelihood classification for digital amplitude-phase modulations. *IEEE Transactions on Communications, 48*, 189–193.
5. Polydoros, A., & Kim, K. (1990). On the detection and classification of quadrature digital modulations in broad-band noise. *IEEE Transactions on Communications, 38*, 1199–1211.
6. Dobre, O. A., & Hameed, F. (2006). Likelihood-based algorithms for linear digital modulation classification in fading channels. In *Proceedings IEEE Canadian Conference on Electrical and Computer Engineering* (pp. 1347–1350).
7. Abdi, A., Dobre, O. A., Choudhry, R., Bar-Ness, Y., & Su, W. (2004). Modulation classification in fading channels using antenna arrays. In *Proceedings of IEEE MILCOM* (pp. 211–217).
8. Swami, A., & Sadler, B. (2000). Hierarchical digital modulation classification using cumulants. *IEEE Transactions on Communications, 48*, 416–429.
9. Marchard, P., Lacoume, J. L., & Le Martret, C. (1998). Multiple hypothesis classification based on cyclic cumulants of different orders. In *Proceedings of IEEE ICASSP* (pp. 2157–2160).
10. Spooner, C. M. (1995). Classification of cochannel communication signal using cyclic cumulants. In *Proceedings of IEEE ASILOMAR* (pp. 531–536).
11. Spooner, C. M. (2001). On the utility of sixth-order cyclic cumulants for RF signal classification. In *Proceedings of IEEE ASILOMAR* (pp. 890–897).
12. Dobre, O. A., Bar-Ness, Y., & Su, W. (2004). Robust QAM modulation classification algorithm using cyclic cumulants. In *Proceedings of IEEE WCNC* (pp. 745–748).
13. Dobre, O. A., Rajan, S., & Inkol, R. (2007). A novel algorithm for blind recognition of M-ary frequency shift keying modulation. In *Proceedings of IEEE WCNC* (pp. 520–524).
14. Dobre, O. A., Zhang, Q., Rajan, S., & Inkol, R. (2008). Second-order cyclostationarity of cyclically prefixed single carrier linear digital modulations with applications to signal recognition. In *Proceedings of IEEE GLOBECOM* (pp. 1–5).
15. Oner, M., & Jondral, F. (2007). On the extraction of the channel allocation information in spectrum pooling system. *IEEE Journal on Selected Areas in Communications, 25*, 558–565.
16. Dobre, O. A., Bar-Ness, Y., & Su, W. (2003). Higher-order cyclic cumulants for high order modulation classification. In *Proceedings of IEEE MILCOM* (pp. 112–117).
17. Dobre, O. A., Abdi, A., Bar-Ness, Y., & Su, W. (2005). Selection combining for modulation recognition in fading channels. In *Proceedings of IEEE MILCOM* (pp. 2499–2505).
18. Boudreau, D., Dubuc, C., Patenaude, F., Dufour, M., Lodge, J., & Inkol, R. (2000). A fast automatic modulation recognition algorithm and its implementation in a spectrum monitoring application. In *Proceedings of IEEE MILCOM* (pp. 732–736).
19. Nikias , C. L., & Petropolu, A. (1993). *Higher-order spectra analysis: A nonlinear signal processing framework*. NJ: Prentice-Hall.
20. Spooner, C. M. (1992). Higher-order statistics for nonlinear processing of cyclostationary signals. In W. A Gardner (Ed.), *Cyclostationarity in communications and signal processing* (pp. 91–167). New York: IEEE Press.
21. Spooner, C. M., & Gardner, W. A. (1994). The cumulant theory of cyclostationary time-series, part II: Development and applications. *IEEE Transactions on Signal Processing, 42*, 3409–3429.

22. Proakis, J. G. (2001). *Digital communications* (4th ed.). New York: Mc-Graw Hill.
23. Napolitano, A. (1995). Cyclic higher-order statistics: Input/output relations for discrete- and continuous-time MIMO linear almost-periodically time-variant systems. *Signal Processing, 42*, 147–166.
24. Schawartz, M., Benett, W. R., & Stein, S. (1996). *Communication systems and techniques*. New York: IEEE Press.
25. Stuber, G. L. (2001). *Principles of mobile communication* (2nd ed.). Boston, MA: Kluwer.
26. Dandawate, V., & Giannakis , G. B. (1995). Asymptotic theory of mixed time averages and *k*th-order cyclic-moment and cumulant statistics. *IEEE Transactions on Information Theory, 41*, 216–232.
27. Ciblat, P., Loubaton, P., Serpedin, E., & Giannakis , G. B. (2002). Asymptotic analysis of blind cyclic correlation-based symbol-rate estimators. *IEEE Transactions on Information Theory, 48*, 1922–1934.

Author Biographies

Octavia A. Dobre received the D. Eng. and Ph.D. degrees in Electrical Engineering from the Polytechnic University of Bucharest, Romania, in 1991 and 2000, respectively. In 2001 she joined the Wireless Information Systems Engineering Laboratory at Stevens Institute of Technology in Hoboken, NJ, as a Fulbright fellow. Between 2002 and 2005, she was with the Department of Electrical and Computer Engineering at New Jersey Institute of Technology (NJIT) in Newark, NJ, as a Research Associate. Since 2005 she has been an Assistant Professor with the Faculty of Engineering and Applied Science at Memorial University of Newfoundland, Canada. Her current research interests include blind modulation classification and parameter estimation, cognitive radio, multiple antenna systems, multicarrier modulation techniques, cyclostationarity applications in communications and signal processing, and resource allocation in emerging wireless networks. Dr. Dobre is an Associate Editor for the IEEE Communications Letters, and has served as the Chair of the Signal Processing and Multimedia Symposium of the 2009 IEEE CCECE (Canadian Conference on Electrical and Computer Engineering).

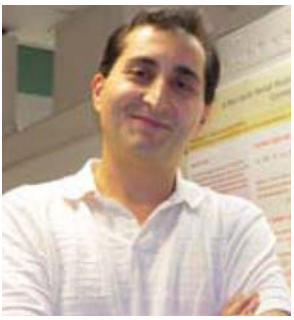

Ali Abdi (S'698, M'601, S'606) received the Ph.D. degree in electrical engineering from the University of Minnesota, Minneapolis, in 2001. He joined the Department of Electrical and Computer Engineering of New Jersey Institute of Technology (NJIT), Newark, in 2001, where he is currently an Associate Professor. His current research interests include characterization and estimation of wireless channels, digital communication in underwater and terrestrial channels, blind modulation recognition, systems biology and molecular networks. Dr. Abdi was an Associate Editor for IEEE Transactions on Vehicular Technology from 2002 to 2007. He was also the co-chair of the Communication and Information Theory Track of the 2008 IEEE ICCCN (International Conference on Computer Communications and Networks). Dr. Abdi has received 2006 NJIT Excellence in Teaching Award, in the category of Excellence in Team, Interdepartmental, Multidisciplinary, or Non-Traditional Teaching. He has also received 2008 New Jersey Inventors Hall of Fame (NJIHoF) Innovators Award on Acoustic Communication, for his work on underwater acoustic communication.

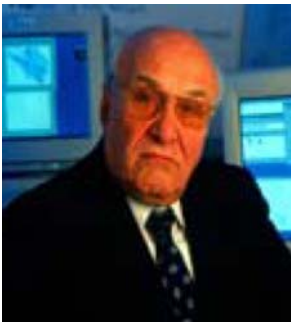

Yeheskel Bar-Ness B.Sc. and M.Sc. degrees in Electrical Engineering from the Technion, Israel, and Ph.D. degree in Applied Mathematics from Brown University, Providence, RI. He is a Distinguished Professor of ECE, Foundation Chair of Communication and Signal Processing Research and Executive Director of the Center for Wireless Communication and Signal Processing Research (CCSPR) at the New Jersey Institute of Technology, Newark. After working in the private sector, he joined the School of Engineering, Tel-Aviv University in 1973. He came to NJIT from AT&T Bell Laboratories in 1985. Current research interests include design of MIMO-OFDM, and MC-CDMA, adaptive array and spatial interference cancellation and signal separation for multi-user communications, and modulation classification. Recently, he is contributing in the area of cooperative communication, modulation classification, cognitive radio, link adaptation with cooperative diversity, cross layer design and analysis and scheduling and beam-forming for downlink with limited feedback. He published numerous papers in these areas. He serves on the editorial board of WIRED Magazine, was the founding Editor-in-chief of IEEE Communication Letters, and was associate and area editor for IEEE Transactions on Communications. He is currently on the editorial board of the Journal of Communication Networks. He has been the technical chair of several major conferences and symposiums and was the recipient of the Kaplan Prize (1973), which is awarded annually by the government of Israel to the ten best technical contributors. He is a Fellow of IEEE and is the recipient of the IEEE Communication Society's "Exemplary Service Award," and was selected the "NJ 2006 Inventor of the Year," recognized for "systems and methods to enhance wireless/mobile communications."

Wei Su received the B.S. degree in electrical engineering and the M.S. degree in systems engineering from Shanghai Jiao Tong University, China, in 1983 and 1987, respectively. He received his M.E., Ph.M., and Ph.D. degrees in electrical engineering from The City University of New York in 1992. He was with US Army Research Laboratory between 1991 and 1996. Currently, he is a senior electronics engineer and technical manager in US Army Communication-Electronics Research Development and Engineering Center (CERDEC) in Fort Monmouth, New Jersey, USA. His research interests include electronic warfare technology, automatic modulation classification, sensor network, cognitive radios, image processing, and adaptive control. He is a recipient of US Army Superior Civilian Service Award and Medal, 2007 IEEE Region I Award, 2004 and 2007 AOC Research and Development Awards, 2005 Army Research and Development Achievement Award, 2002 Thomas Alva Edison Patent Award, Army Material Command Top 10 Employee Nomination, AOC Electronic Warfare Technology Hall of Fame, and US Army CERDEC Inventor's Wall of Honor.